Solar Energy Materials & Solar Cells xxx (xxxx) xxx

Contents lists available at ScienceDirect

Solar Energy Materials and Solar Cells

journal homepage: http://www.elsevier.com/locate/solmat

21.3%-efficient n-type silicon solar cell with a full area rear TiO_x/LiF/Al electron-selective contact

Wenjie Wang [a,b], Jian He [b,d], Di Yan [b], Chris Samundsett [b], Sieu Pheng Phang [b], Zengguang Huang [c], Wenzhong Shen [a,*], James Bullock [d], Yimao Wan [b,**]

[a] Institute of Solar Energy, Key Laboratory of Artificial Structures and Quantum Control (Ministry of Education), School of Physics and Astronomy, Shanghai Jiao Tong University, 800 Dong Chuan Road, Shanghai, 200240, PR China
[b] Research School of Electrical, Energy and Materials Engineering, Australian National University, Canberra, ACT, 0200, Australia
[c] School of Science, Huaihai Institute of Technology, Lianyungang, Jiangsu Province, 222005, PR China
[d] School of Electrical and Electronic Engineering, University of Melbourne, Melbourne, VIC, 3052, Australia

ARTICLE INFO

Keywords:
Electron-selective contact
ALD-TiO_2
High-efficient c-Si solar cell

ABSTRACT

In this work, we investigate an efficient electron-selective passivating contact with TiO_x/LiF/Al contact structure, which offers both low surface recombination and specific contact resistance. Optimized TiO_x layer thickness of 4 nm provides high quality surface passivation, achieving minority carrier lifetime of 3.03 ms on 5 Ω cm n-type wafers, with a saturated current density J_0 of 23 fA/cm^2. In addition, inserting a 1 nm LiF between the 4 nm TiO_x and Al reduces the contact resistivity to 18 mΩ cm^2. The low contact resistivity of TiO_x/LiF/Al contact is attributed to barrier reduction from the low work function of LiF/Al stack. A champion solar cell efficiency of 21.3% has been achieved for an n-type crystalline silicon device with a full-area rear TiO_x/LiF/Al contact, demonstrating the excellent potential of this passivating contact for fabricating high-efficiency silicon solar cells.

1. Introduction

N-type crystalline silicon (n-c-Si) shows a higher tolerance to common metal impurities and no light-induced degradation, which results in higher bulk quality and greater stability compared to p-type crystalline silicon (p-c-Si) [1,2]. As such, many high efficiency silicon solar cells are fabricated on high-quality n-c-Si wafers. Two efficiency recorded n-c-Si solar cells of particular prominence are the 25.7% efficiency solar cell with tunneling oxide passivating contact [3], and 26.7%-efficient silicon heterojunction solar cells (SHJ) with the intrinsic and doped hydrogenated amorphous silicon layers [4]. One of the key factors in obtaining high efficiency is the application of carrier-selective contacts (CSC), which introduces excellent surface passivation and low contact resistivity. In recent years, metal oxide layers have been widely used in c-Si solar cells as CSCs on account of their appropriate band gap and suitable work function, which are able to transmit one type of carriers while blocking the other. For example, thin layers of high work function MoO_x (~5.7 eV) have been used to substitute p-type hydrogenated amorphous silicon layers (p-a-Si:H) as hole selective layers on SHJ solar cells, achieving 22.5% efficiency [5]. Similarly, TiO_x with relatively low work function (~4 eV) have been used as electron-selective layers on conventional silicon solar cells with tunneling oxides, achieving an efficiency of 22.1% [6]. These indicate that metal oxide layers show a great potential for achieving high performance c-Si solar cells.

A large part of the success of TiO_x comes from its ability to provide high carrier selectivity, as shown in the work presented by Yang et al. in 2016 [7], obtaining the efficiency of 19.6% with TiO_x/Al electron-selective contact. However, the TiO_x/Al electron-selective contact behaves poorly in terms of contact resistivity. This limits the efficiency of solar cells, commonly attributed to a large barrier height. Allen et al. [8] investigated the research of replacing the Al with a relatively lower work function metal Ca (~2.9 eV) to acquire lower contact resistivity and realized an efficiency of 21.8% with a partial rear contact structure. As an alternative, a LiF/Al stack with a low work function (~2.8 eV) are widely used in organic photovoltaics to form effective electron transport layers and has recently attracted interest in silicon photovoltaics. It has been shown that the LiF/Al stack performs well in dopant-free asymmetric hetero-contact silicon solar cells, which achieved an efficiency of 19.4% [9]. Moreover, inserting a TiO_x ultrathin layer between an i-a-Si:H passivating layer and LiF significantly

* Corresponding author.
** Corresponding author.
E-mail addresses: wzshen@sjtu.edu.cn (W. Shen), yimao.wan@anu.edu.au (Y. Wan).

https://doi.org/10.1016/j.solmat.2019.110291
Received 29 May 2019; Received in revised form 8 November 2019; Accepted 9 November 2019
0927-0248/© 2019 Elsevier B.V. All rights reserved.

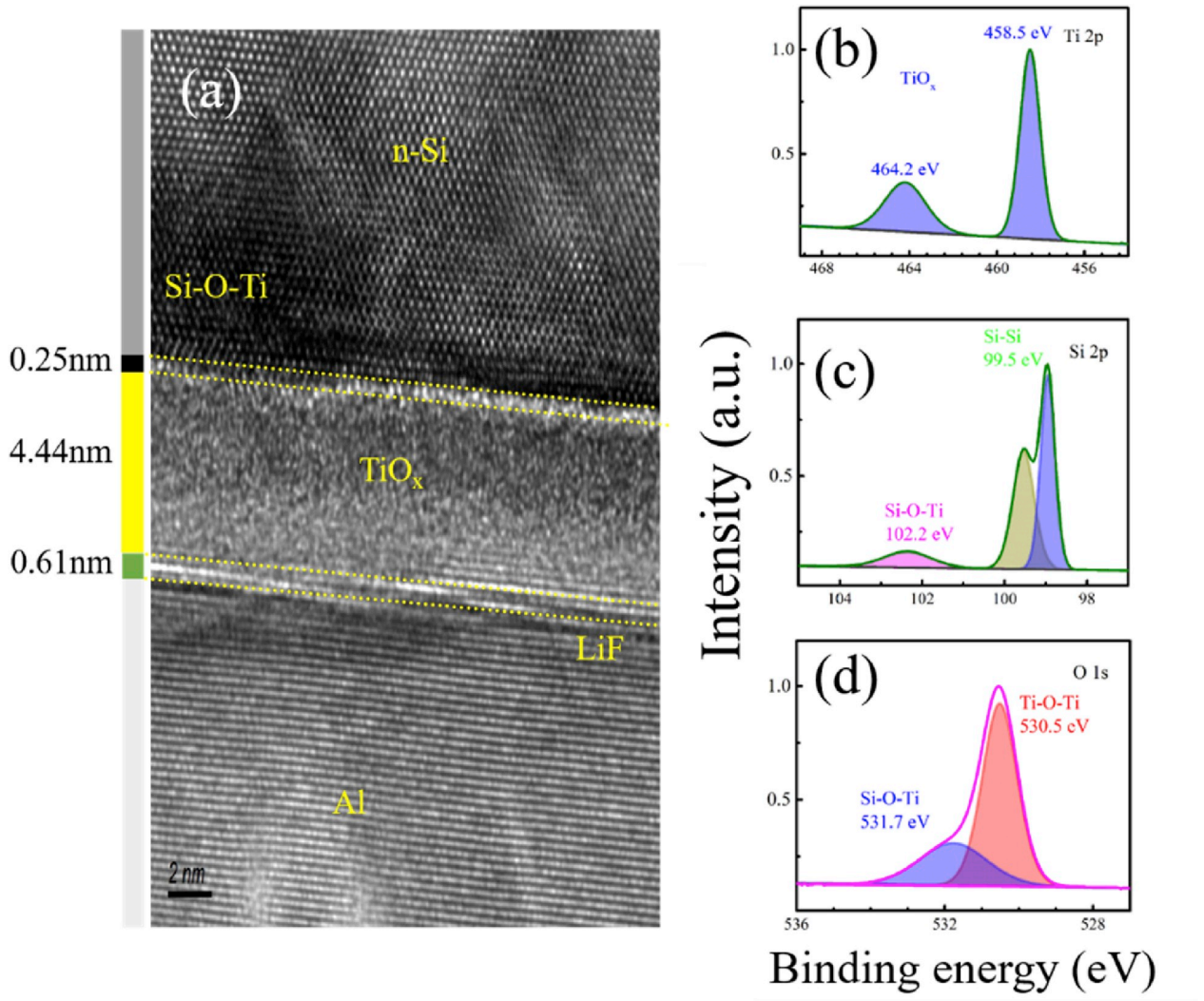

Fig. 1. (a) Cross-sectional TEM images of TiO_x/LiF/Al contact. Normalized X-ray photoelectron spectra of (b) Si (2p) (c) O (1s) and (d) Ti (2p) for Si/TiO_x interfaces with the TiO_x/LiF/Al contact.

enhanced the efficiency by 1.3% [10]. The latest work shows the TiO_x/LiF/Al stack enhances the efficiency of cells, enabling over 23% with the partial rear contact structure, demonstrating the great potential of the TiO_x/LiF/Al stack as electron-selective passivating contacts [11].

In this work, we investigated the combination of low work function LiF/Al stack with passivating TiO_x layer to obtain both good surface passivation and low contact resistivity. The optimized electron-selective passivating contact was applied as full-area rear contact in c-Si solar cell, resulting in efficiency of 21.3%.

2. Experimental

N-type (100)-oriented Fz silicon wafers (400 μm, 5 Ω cm) were used for passivation measurement while n-type (100)-oriented Cz silicon wafers (290 μm, 0.1 Ω cm) were utilized for contact resistivity measurements. For surface passivation measurements, the wafers were damaged etched, RCA cleaned and dipped in dilute HF solution, prior to deposition of TiO_x layers. Different thicknesses by atomic layer deposition (ALD, TFS 200, BENEQ, Finland) at 230 °C were deposited on both sides of wafers. The deposition precursors Titanium Tetrakis Isopropoxide (TTIP) and H_2O were used. The excess carrier lifetimes were measured via quasi-steady-state photoconductance (QSSPC) using a Sinton Instruments WCT120 photoconductance tester and the lifetimes were recorded at excess minority carrier density of 1×10^{15} cm^{-3}. For the contact resistivity measurement, LiF/Al stacks (~1 nm/100 nm) were thermally evaporated on wafers with a single side TiO_x deposition. The contact resistivity was extracted using the Cox and Strack method [12]. After deposition, the effect of annealing in N_2 ambient was investigated by varying the annealing time at 250 °C and also by varying the annealing temperature for fixed annealing time of 5 min. Samples with TiO_x/LiF/Al contacts (~5 nm/1 nm/100 nm) where TiO_x has been annealed in N_2-gas ambient at 250 °C for 5 min were prepared for transmission electron microscopy (TEM) and X-ray photoelectron spectra (XPS).

The solar cells were fabricated on 1 Ω cm n-type Cz silicon wafers, with random pyramid texturing on the front side. Boron diffusion was used to form the p + layers on the front side, which were then coated by an Al_2O_3/SiN_x stack for surface passivation and anti-reflection coating. The front electrodes were deposited by thermal evaporation of Cr/Pd/Ag and following silver electroplating was used to further thicken the front electrodes. On the rear side, the electrode was fully covered by TiO_x/LiF/Al. The final size of the solar cells is 2×2 cm^2. The light *J-V* measurement was taken under a solar simulator providing standard AM1.5 g illumination and external quantum efficiency (EQE), internal quantum efficiency (IQE) and reflection was extracted from a quantum efficiency measurement system (QEX10, PV measurements, USA) in air without bias light.

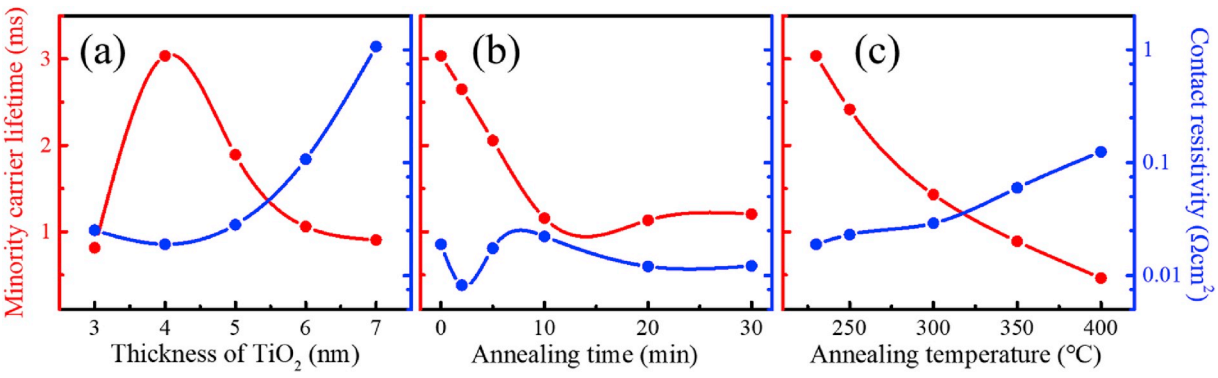

Fig. 2. Variation of the minority carrier lifetime and contact resistance as a function of (a) thickness as deposited (b) annealing time at the temperature of 250 °C (c) annealing temperature for 5 min.

3. Result and discussion

The interfacial layer features of TiO_x/LiF/Al contact were characterized by TEM and XPS, as depicted in Fig. 1. In Fig. 1(a), different layers with measured thickness are visualized clearly by TEM due to different material structure. An interfacial layer with a thickness of about 0.25 nm could be observed between silicon substrate and TiO_x, which has an impact on surface passivation and the corresponding contact resistance. In order to further study the interfacial layer between Si and TiO_x, XPS measurement was applied to this contact structure. Fig. 1(b), (c) and (d) present the binding energy of Ti, Si and O elements respectively. According to the XPS analysis as shown in Fig. 2(b), there are the typical binding energies for Ti (4^+) with the splitting spin-orbit energy of 5.7 eV, which indicates that there is no discernible signal for any lower valent Ti species [8,13,14]. The binding energy of 102.2 eV was observed in the Si spectrum at the interfacial region, as shown in Fig. 2(c), which is different from conventional O–Si–O binding energy of 102.9 eV [13–15]. A peak with 531.7 eV is found in O (1s) spectrum in Fig. 2(c), other than the Si–O–Si binding energy of 532.2 eV as shown in Refs. [13,14]. These signals indicate that the bonds Si–O–Ti should exist in the interfacial layer between silicon and TiO_x [15]. Moreover, the ratio of the relative atomic percentage of the Ti and O is calculated as 1:2.2 by XPS analysis, which is not in agreement with the stoichiometry ratio of 1:2. It is speculated that the O is not only combined with Ti to form the stoichiometry TiO_x but also forms bonds with Si in the interfacial layer. Thus, it is concluded that the interfacial layer is an alloy of SiO_x and TiO_x [14]. The alloy might be either formed in the first cycles of ALD process or in the annealing process. The formation of a sub-stoichiometric SiO_x layer is standard for ALD deposited metal oxides e.g., AlO_x.

The measured minority carrier lifetimes and contact resistivity values as a function of TiO_x thickness are shown in Fig. 2(a). It can be observed that both the best passivation quality and the lowest contact resistivity are achieved for TiO_x with 4 nm thickness, effective lifetime of 3.03 ms and contact resistivity of 18 mΩ cm^2 were obtained. The surface recombination current density J_0 is extracted to be 23 fA/cm^2. On the other hand, a thin TiO_x layers, e.g. 3 nm TiO_x, is too thin to provide stable passivation while the phase transition of TiO_x from amorphous phase to anatase phase could be caused by increased crystallization for thicker films, as suggested by Ref. [16]. As a result, degradation of surface passivation was observed, as shown in Fig. 2(a). In addition, the contact resistivity increases significantly with the increasing thickness due to the bulk resistivity of amorphous TiO_x.

The critical parameters in the post annealing process in N_2 ambient of as-deposited ALD-TiO_2 are annealing time and annealing temperature, as shown in Fig. 2(b) and (c). Fig. 2(b) exhibits that at the same annealing temperature of 250 °C, increasing the annealing time to 30 min has a negative influence on passivation, reducing the minority carrier lifetime from 3.03 ms to 1.20 ms. On the other hand, the contact resistivity is not sensitive to the annealing time. Although annealing of amorphous TiO_x at 250 °C does not cause phase transition to anatase phase [17], intermixing at the interface between Si and TiO_x might play an important role in surface passivation, and may lead to a greater density of interface states with annealing time.

The dependence of surface passivation qualities and contact resistivity of TiO_x values on the annealing temperature within the same time of 5 min is shown in Fig. 2(c). The high annealing temperature (>300 °C) induces the phase transition of TiO_x which leads to a sharp degradation of passivation from 3.03 ms to 0.463 ms at 400 °C [6,16,17]. The results also show an increase in contact resistivity with increasing annealing temperature. However, the increase in contact resistivity values is not expected because the bulk conductivity of TiO_x is increased after the phase transition. The possible explanation of this effect is the increasing thickness of the mixed material region with the

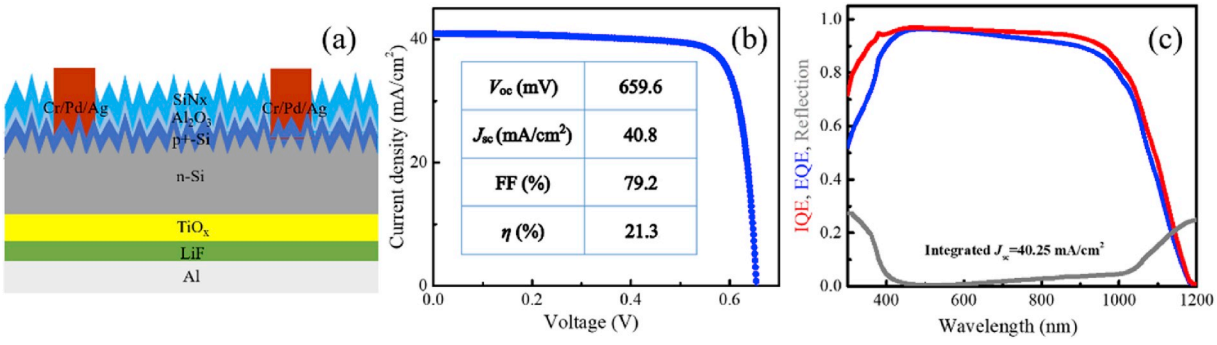

Fig. 3. (a) Schematic of n-c-Si cell with a full-area rear passivating, electron-selective TiO_x/LiF/Al contact. (b) Light *J–V* curves under a standard AM1.5 g illumination and electrical parameters of cells with full area rear TiO_x/LiF/Al contact. (c) EQE, IQE and reflection of the cell.

annealing temperature rising, which increases insulating property, thus impeding the electron transport.

Finally, the TiO_x with an optimized thickness of 4 nm has been applied on the solar cell structure as shown in Fig. 3(a). An efficiency of 21.3% has been achieved with V_{oc} (open-circuit voltage) = 659.6 mV, J_{sc} (short-circuit current density) = 40.8 mA/cm^2 and FF (fill factor) = 79.2%, as shown in the inset table of Fig. 3(b). Compared to the cells with a full area rear TiO_x/Al contact fabricated by Yang et al. [7], the efficiency is 1.7% higher, which proves the high performance of TiO_x/LiF/Al contact. The 27 mV higher V_{oc} and 1.5 mA/cm^2 higher J_{sc} show the better passivation. The corresponding EQE, IQE and reflection spectra are presented in Fig. 3(c). The uniform texturing and excellent anti-reflection layers contribute to the low reflection and enhanced absorption of the cell in the range of the solar spectrum. For wavelength between 400 nm to 900 nm, the EQE value remains higher than 90%, which indicates that most of phonons in this wavelength range are absorbed and extracted to external circuit, improving the current density. The integration of the EQE and the solar spectrum product shows the value of J_{sc} up to 40.25 mA/cm^2, in agreement with J_{sc} given by the efficiency measurement.

4. Conclusion

This paper describes an electron-selective passivating contact TiO_x/LiF/Al structure with both good passivation and low contact resistivity. Characterization of the interfacial layer of Si/TiO_x shows high density of the mixture of SiO_x and TiO_x, which has a critical effect on the passivation and contact resistivity. The impact of the TiO_x layer thickness, annealing times and annealing temperatures was investigated. It is clear that as-deposited 4 nm TiO_x is the optimized thickness that results in an effective lifetime of 3.03 ms with a low saturated current density J_0 of 23 mA/cm^2 and a contact resistivity of 18 mΩ cm^2. The high efficiency of 21.3% has been achieved in Si solar cell with a full area TiO_x/LiF/Al rear contact, which shows a great potential for fabrication of high efficiency solar cell.

Credit author statement

Wenjie Wang: Conceptualization, Investigation, Visualization, Writing - Original Draft, Writing - Review & Editing

Jian He: Investigation, Writing - Review & Editing.

Di Yan: Investigation, Writing - Review & Editing.

Chris Samundsett: Investigation, Writing - Review & Editing.

Sieu Pheng Phang: Investigation, Writing - Review & Editing.

Zengguang Huang: Investigation, Writing - Review & Editing.

Wenzhong Shen: Conceptualization, Supervision, Project administration, Funding acquisition, Writing - Review & Editing.

James Bullock: Conceptualization, Investigation, Writing - Review & Editing.

Yimao Wan: Conceptualization, Supervision, Project administration, Writing - Review & Editing, Funding acquisition.

Declaration of competing interest

The authors declare that they have no known competing financial interests or personal relationships that could have appeared to influence the work reported in this paper.

Acknowledgements

This work was supported by the Major State Basic Research Development Program of China (No. 2018YFB1500501), National Natural Science Foundation of China (Nos. 11834011, 11674225, 61774069 and 11974242), and China Scholarship Council (CSC) funding. J.H. and Y.W. acknowledge the support of the Australian Renewable Energy Agency (ARENA) Research and Development Program (2017/RND007).

Appendix A. Supplementary data

Supplementary data to this article can be found online at https://doi.org/10.1016/j.solmat.2019.110291.

References

[1] Y. Wan, C. Samundsett, D. Yan, T. Allen, J. Peng, J. Cui, X. Zhang, J. Bullock, A. Cuevas, A magnesium/amorphous silicon passivating contact for n-type crystalline silicon solar cells, Appl. Phys. Lett. 109 (2016) 113901, https://doi.org/10.1063/1.4962960.

[2] D. MacDonald, The emergence of n-type silicon for solar cell manufacture. In 50th Annual AuSES Conference (Solar 2012), Melbourne, Australia.

[3] A. Richter, J. Benick, F. Feldmann, A. Fell, M. Hermle, S.W. Glunz, n-Type Si solar cells with passivating electron contact: identifying sources for efficiency limitations by wafer thickness and resistivity variation, Sol. Energy Mater. Sol. Cells 173 (2017) 96–105, https://doi.org/10.1016/j.solmat.2017.05.042.

[4] K. Yoshikawa, W. Yoshida, T. Irie, H. Kawasaki, K. Konishi, H. Ishibashi, T. Asatani, D. Adachi, M. Kanematsu, H. Uzu, K. Yamamoto, Exceeding conversion efficiency of 26% by heterojunction interdigitated back contact solar cell with thin film Si technology, Sol. Energy Mater. Sol. Cells 173 (2017) 37–42, https://doi.org/10.1016/j.solmat.2017.06.024.

[5] J. Geissbühler, J. Werner, Martin De Nicolas, L. Barraud, A. Hessler-Wyser, M. Despeisse, S. Nicolay, A. Tomasi, B. Niesen, S. De Wolf, C. Ballif, 22.5% efficient silicon heterojunction solar cell with molybdenum oxide hole collector, Appl. Phys. Lett. 107 (2015), https://doi.org/10.1063/1.4928747, 081601.

[6] X. Yang, K. Weber, Z. Hameiri, S. De Wolf, Industrially feasible, dopant-free, carrier-selective contacts for high-efficiency silicon solar cells, Prog. Photovolt. Res. Appl. (2017) 896–904, https://doi.org/10.1002/pip.2901.

[7] X. Yang, P. Zheng, Q. Bi, K. Weber, Silicon heterojunction solar cells with electron selective TiOx contact, Sol. Energy Mater. Sol. Cells 150 (2016) 32–38, https://doi.org/10.1016/j.solmat.2016.01.020.

[8] T.G. Allen, J. Bullock, Q. Jeangros, C. Samundsett, Y. Wan, J. Cui, A. Hessler-Wyser, S. De Wolf, A. Javey, A. Cuevas, A low resistance calcium/reduced titania passivated contact for high efficiency crystalline silicon solar cells, Adv. Energy Mater. (2017) 1602606, https://doi.org/10.1002/aenm.201602606.

[9] J. Bullock, M. Hettick, J. Geissbühler, A.J. Ong, T. Allen, C.M. Sutter-Fella, T. Chen, H. Ota, E.W. Schaler, S. De Wolf, C. Ballif, A. Cuevas, A. Javey, Efficient silicon solar cells with dopant-free asymmetric heterocontacts, Nat. Energy 1 (2016) 15031, https://doi.org/10.1038/NENERGY.2015.31.

[10] J. Bullock, Y. Wan, Z. Xu, S. Essig, M. Hettick, H. Wang, W. Ji, M. Boccard, A. Cuevas, C. Ballif, A. Javey, Stable dopant-free asymmetric heterocontact silicon solar cells with efficiencies above 20%, ACS Energy Lett. 3 (2018) 508–513, https://doi.org/10.1021/acsenergylett.7b01279.

[11] J. Bullock, Y. Wan, M. Hettick, Z. Xu, S.P. Phang, D. Yan, H. Wang, W. Ji, C. Samundsett, Z. Hameiri, D. Macdonald, A. Cuevas, A. Javey, Dopant-free partial rear contacts enabling 23% silicon solar cells, Adv. Energy Mater. (2019) 1803367, https://doi.org/10.1002/aenm.201803367.

[12] R. Cox, H. Strack, Ohmic contacts for GaAs devices, Solid State Electron. (1967) 1213–1218, https://doi.org/10.1016/0038-1101(67)90063-9.

[13] G. Sahasrabudhe, S.M. Rupich, J. Jhaveri, A.H. Berg, K.A. Nagamatsu, G. Man, Y. J. Chabal, A. Kahn, S. Wagner, J.C. Sturm, J. Schwartz, Low-temperature synthesis of a TiO_2/Si heterojunction, J. Am. Chem. Soc. (2015) 14842–14845, https://doi.org/10.1021/jacs.5b09750.

[14] J. He, Z. Ling, P. Gao, J. Ye, TiO_2 films from the low-temperature oxidation of Ti as passivating-contact layers for Si heterojunction solar cells, Sol. RRL (2017) 1700154, https://doi.org/10.1002/solr.201700154.

[15] R.P. Netterfield, P.J. Martin, C.G. Pacey, W.G. Sainty, D.R. McKenzie, G. Auchterlonie, Ion-assisted deposition of mixed TiO_2-SiO_2 films, J. Appl. Phys. (1989) 1805–1809, https://doi.org/10.1063/1.344352.

[16] I. Yu, I. Chang, H. Cheng, Y. Lin, Surface passivation of c-Si by atomic layer deposition TiO2 thin films deposited at low temperature, in: Proceedings of the 40th IEEE Photovoltaics Specialist Conference, Denver, 2014, pp. 1271–1274.

[17] B. Liao, B. Hoex, A.G. Aberle, D. Chi, C.S. Bhatia, Excellent c-Si surface passivation by low-temperature atomic layer deposited titanium oxide, Appl. Phys. Lett. 104 (2014) 253903, https://doi.org/10.1063/1.4885096.